DOI: 10.1002/chem.200500778

An Investigation of Lanthanum Coordination Compounds by Using Solid-State ^{139}La NMR Spectroscopy and Relativistic Density Functional Theory

Mathew J. Willans, Kirk W. Feindel, Kristopher J. Ooms, and Roderick E. Wasylishen*[a]

Abstract: Lanthanum-139 NMR spectra of stationary samples of several solid La^{III} coordination compounds have been obtained at applied magnetic fields of 11.75 and 17.60 T. The breadth and shape of the ^{139}La NMR spectra of the central transition are dominated by the interaction between the ^{139}La nuclear quadrupole moment and the electric field gradient (EFG) at that nucleus; however, the influence of chemical-shift anisotropy on the NMR spectra is non-negligible for the majority of the compounds investigated. Analysis of the experimental NMR spectra reveals that the ^{139}La quadrupolar coupling constants (C_Q) range from 10.0 to 35.6 MHz, the spans of the chemical-shift tensor (Ω) range from 50 to 260 ppm, and the isotropic chemical shifts (δ_{iso}) range from −80 to 178 ppm. In general, there is a correlation between the magnitudes of C_Q and Ω, and δ_{iso} is shown to depend on the La coordination number. Magnetic-shielding tensors, calculated by using relativistic zeroth-order regular approximation density functional theory (ZORA-DFT) and incorporating scalar only or scalar plus spin–orbit relativistic effects, qualitatively reproduce the experimental chemical-shift tensors. In general, the inclusion of spin–orbit coupling yields results that are in better agreement with those from the experiment. The magnetic-shielding calculations and experimentally determined Euler angles can be used to predict the orientation of the chemical-shift and EFG tensors in the molecular frame. This study demonstrates that solid-state ^{139}La NMR spectroscopy is a useful characterization method and can provide insight into the molecular structure of lanthanum coordination compounds.

Keywords: density functional calculations · lanthanum · magnetic-shielding tensors · NMR spectroscopy · quadrupolar coupling constants

Introduction

The coordination chemistry of the lanthanides (Ln) is extremely diverse, with Ln^{III} metals forming complexes with numerous oxygen- and nitrogen-donating ligands in which the metal adopts a wide variety of coordination numbers.[1–3] This chemical and structural variety has been exploited and Ln coordination compounds have found use in biology as molecular-recognition and chirality-sensing agents[4] as well as DNA hydrolysis promoters,[5] in NMR as shift reagents[6–8] and in magnetic resonance imaging (MRI) as contrast agents,[9–11] in organic synthesis as reagents and catalysts,[12–15] and as luminescent sensors and light converters.[16,17]

The study of Ln coordination compounds by means of NMR spectroscopy is difficult because the majority of the compounds are paramagnetic. Given that the unpaired spin density in these complexes is generally localized on the metal, high-resolution NMR spectra of spin-active lanthanide isotopes are often impossible to obtain. Fortunately, paramagnetic Ln compounds frequently have diamagnetic La^{III} analogues that are amenable to study by NMR spectroscopy. As a result of La having an isotope with favorable NMR properties—^{139}La, $I=7/2$ (I=nuclear spin), natural abundance of 99.9%, $\Xi=14.125\%$ (Ξ=ratio of the ^{139}La frequency to that of ^{1}H in tetramethylsilane in the same magnetic field), and a moderate nuclear quadrupole moment ($Q=+20$ fm^2)[18]—numerous ^{139}La solution NMR studies have been reported.[19] In spite of the large number of solution ^{139}La NMR studies that have been performed, there are limitations of the technique that one must consider. Often the solubility of La compounds is low, which can

[a] M. J. Willans, K. W. Feindel, K. J. Ooms, Prof. R. E. Wasylishen
Department of Chemistry
Gunning/Lemieux Chemistry Centre
University of Alberta
Edmonton, AB, T6G 2G2 (Canada)
Fax: (+1) 780-492-8231
E-mail: roderick.wasylishen@ualberta.ca

Supporting information for this article is available on the WWW under http://www.chemeurj.org/ or from the author.

lead to long experimental times or prevent solution NMR studies completely. When solubility is not an issue, efficient nuclear quadrupolar relaxation of ^{139}La in isotropic solutions results in broadened NMR peaks. In addition, rapid ligand exchange in solution can introduce ambiguity in the identity of the compound, leading to a discrepancy between structural information garnered from single-crystal diffraction studies and solution NMR experiments. When NMR experiments are conducted on solid samples, however, one can be confident that the structure of the sample under investigation is identical to that determined by single-crystal diffraction data when available.

The most dramatic difference between solution and solid-state NMR of a quadrupolar nucleus such as ^{139}La is that the linewidth of the NMR spectra of powder samples is generally limited not by relaxation but by the orientation-dependence of the quadrupolar interaction. The interaction of the quadrupole moment of the nucleus with the electric field gradient (EFG) at that nucleus constitutes the quadrupolar interaction. In some instances, the orientation-dependence of the magnetic-shielding interaction also contributes to the breadth of the NMR spectrum. Characterization of the EFG and magnetic-shielding tensors obtained from NMR spectra can yield information about the local symmetry at the quadrupolar nucleus.[20–22] Given the high NMR receptivity of ^{139}La and that structural information can be obtained from solid-state NMR spectra of quadrupolar nuclei, it is surprising that relatively few NMR studies of solid diamagnetic La compounds have been performed. Such studies have been limited to characterizing inorganic materials[23–28] and simple inorganic salts;[23,29–32] however, no ^{139}La NMR studies of solid coordination compounds have been reported.

Our goal is to investigate the feasibility of using solid-state ^{139}La NMR spectroscopy to study lanthanum coordination compounds. In particular, can relationships between NMR parameters and molecular structure be derived? To accomplish these goals, a wide variety of well-characterized La^{III} model compounds, comprised of either oxygen-donating or both oxygen- and nitrogen-donating ligands, have been chosen. The La coordination number in the compounds examined ranges from 8 to 12 (Table 1), as determined by single-crystal X-ray diffraction studies.[33–42] To analyze the ^{139}La NMR spectra of these compounds, experiments were performed on stationary powder samples at moderate and high applied magnetic fields of 11.75 T (ν_L(^{139}La) = 70.7 MHz) and 17.60 T (ν_L(^{139}La) = 105.9 MHz). The use of two applied magnetic fields and the variety of La coordination compounds studied allows one to determine the range of NMR observables in these compounds. Theoretical calculations of ^{139}La magnetic-shielding and EFG tensors were performed in order to assess the ability of the zeroth-order regular approximation density functional theory (ZORA-DFT) method to reproduce the experimental NMR parameters and to suggest orientations of the EFG and shielding tensors in the molecular frame.

Results and Discussion

Solid-state ^{139}La NMR: In practice, when performing solid-state NMR experiments on half-integer quadrupolar nuclei with moderate quadrupole moments such as ^{139}La, one generally acquires only the spectrum of the central, $m_I = {}^1/_2 \leftrightarrow m_I = -{}^1/_2$ (m_I = magnetic quantum number of the nuclear spin), transition.[43,44] Usually only the ^{139}La central transi-

Table 1. Lanthanum(III) coordination compounds included in this study.

	Abbreviated name[a]	Structural formula	CN[b]	Coordination geometry[c]	Ligands[d]	Use/Interest/Related Ln^{III} complexes
1	$[La(acac)_3(H_2O)_2]$	$[La(C_5H_7O_2)_3(H_2O)_2]$	8[33]	square antiprism	OB, OU	Ln acac derivatives used as NMR shift reagents;[6–8] analogous Nd complex[75]
2	$[La(bipyO)_4(ClO_4)_3]$	$[La(C_{10}H_8N_2O_2)_4(ClO_4)_3]$	8[34]	cube	OB	analogous Nd and Lu complexes[76]
3	$[La(Ph_2MePO)_3(NO_3)_3]$	$[La(C_6H_5)_2CH_3PO)_3(NO_3)_3]$	9[35]	tricapped trigonal prism	OU, OB	numerous similar compounds[35]
4	$[La(mal)_2(H_2O)_2]\cdot H_2O$	$[La(C_3H_2O_4)(C_3H_3O_4)(H_2O)_2]\cdot H_2O$	9[36]	monocapped square antiprism	OB, OU	polymeric carboxylate; similar Nd,[77,78] Eu,[79] and Gd[80] complexes
5	$[La(phen)_2(NO_3)_3]$	$[La(C_{12}H_8N_2)_2(NO_3)_3]$	10[37]	bicapped dodecahedron	NB, OB	numerous analogous complexes[81–86]
6	$[La(glut)_2(H_2O)]\cdot H_2O$	$[La(C_5H_6O_4)(C_5H_7O_4)(H_2O)]\cdot H_2O$	10[38]	bicapped dodecahedron	OB, OU	polymeric carboxylate; numerous similar complexes[87,88]
7	$[La(teg)(NO_3)_3]$	$[La(C_8H_{18}O_5)(NO_3)_3]$	11[39]	tricapped cube	OP, OB	acyclic ligand used as a crown-ether analogue; analogous Nd complex[89]
8	$[La([15]crown-5)(NO_3)_3]$	$[La(C_{10}H_{20}O_5)(NO_3)_3]$	11[40]	monocapped pentagonal antiprism	OM, OB	crown-ether ligand used to complex metals;[90] analogous Ce,[91] Eu,[92] and Pr[93] complexes
9	$[La([18]crown-6)(NO_3)_3]$	$[La(C_{12}H_{24}O_6)(NO_3)_3]$	12[41]	icosehedron	OM, OB	analogous Pr complex[94]
10	$[La(N\text{-}macro)(NO_3)_3]$	$[La(C_{22}H_{26}N_6)(NO_3)_3]$	12[42]	bicapped pentagonal prism	NM, OB	numerous similar complexes[95–98]

[a] acac = acetylacetonate, bipyO = 2,2′-bipyridine-1,1′-dioxide, phen = 1,10-phenanthroline, mal = malonic acid, glut = glutamic acid, TEG = tetraethyleneglycol, N-macro = di(ethane-1,2-diyl)bis(pyridine-2,6-diacetimine). [b] CN = coordination number as determined by single-crystal X-ray diffraction studies. See text for a discussion of the CN in **4**. [c] All compounds are distorted from these idealized polyhedra. [d] OU = O-donating unidentate, OB = O-donating bidentate, NB = N-donating bidentate, OP = O-donating pentadentate, OM = O-donating macrocycle, NM = N-donating macrocycle.

tion is observable in a single NMR experiment as the satellite transitions are spread over several hundred kilohertz. The lineshape of ^{139}La central-transition NMR spectra depends primarily on the magnitudes of the principal components of the EFG tensor, which are ordered such that $|V_{ZZ}| \geq |V_{YY}| \geq |V_{XX}|$. In addition, the principal components of the chemical-shift tensor, defined such that $\delta_{11} \geq \delta_{22} \geq \delta_{33}$, and the relative orientation of EFG and chemical-shift tensors may also influence the ^{139}La NMR lineshape.[45,46] The EFG tensor is described by the nuclear quadrupolar coupling constant, $C_Q = eQV_{ZZ}h^{-1}$, where e is the elementary charge, Q is the nuclear quadrupole moment, and h is the Planck constant, and the asymmetry parameter, $\eta_Q = (V_{XX}-V_{YY})/V_{ZZ}$, which is restricted to values between 0 and 1. The chemical-shift tensor is described by the isotropic chemical shift ($\delta_{iso} = (\delta_{11}+\delta_{22}+\delta_{33})/3$), the span ($\Omega = \delta_{11}-\delta_{33}$), and the skew ($\kappa = 3(\delta_{22}-\delta_{iso})\Omega^{-1}$), which is restricted to values between -1 and $+1$.[47] The relative orientation of the EFG and chemical-shift tensors is defined by the Euler angles—α, β, and γ—and thus a total of eight parameters describe the NMR spectra, theoretical examples of which are presented in Figure 1. The principal components of the chemical-shift tensor are related to those of the magnetic-shielding tensor by $\delta_{ii} = (\nu_{ii}-\nu_{ref})/\nu_{ref} \approx \sigma_{ref}-\sigma_{ii}$, in which ν_{ref} and σ_{ref} are the frequency and absolute isotropic magnetic-shielding constant of a reference sample, respectively. Similarly, ν_{ii} are the frequencies corresponding to the principal components of the magnetic-shielding tensor σ_{ii} ($i = 1$, 2, or 3) of the compound under investigation. However, the span (Ω) and skew (κ) are defined such that their values are equivalent for both the magnetic-shielding and chemical-shift tensors. The maximum possible orientation-dependence of the chemical shift, Ω, is sometimes referred to as the chemical-shift anisotropy, CSA.

Typical experimental ^{139}La NMR spectra of solid lanthanum(III) coordination compounds at applied magnetic fields of 11.75 and 17.60 T can be found in Figures 2–5. To extract the NMR parameters that determine the lineshapes of these spectra, one can take advantage of the fact that the influence of the second-order quadrupolar interaction decreases with increasing magnetic field strength whereas the CSA (in Hz) is directly proportional to the magnetic field strength. Thus, the different lineshapes observed for the ^{139}La central transition at 11.75 and 17.60 T are of critical importance for accurate simulation of the experimental spectra (see Figures 2–5 and Table 2). All the compounds studied have small ^{139}La CSAs and thus the breadth and general shape of the NMR spectra are dictated primarily by the second-order quadrupolar interaction.[43,44] The ^{139}La C_Q values measured range from 10.0 to 35.6 MHz with η_Q values spanning the possible range from 0 to 1. The magnitude of the C_Q values are similar to those reported in the few ^{139}La solid-state NMR studies that have been performed on diamagnetic La compounds.[23,24,30,32] To date, the largest recorded ^{139}La C_Q value is 144 MHz, which was reported for gaseous La^{I}F and obtained by using high-resolution microwave spectroscopy.[48] The ^{139}La C_Q values reported here are thus relatively small, however, the largest C_Q values are approaching the current limit at which solid-state NMR can be used to measure C_Q for an $I = 7/2$ nucleus in a single experiment at moderate applied magnetic fields using standard NMR probes.

A unique feature of the ^{139}La NMR spectra presented in this study is that Ω of the chemical-shift tensor could be determined for the majority of compounds investigated (see Table 2). CSA parameters were not reported in early ^{139}La NMR studies of diamagnetic compounds[23,24,30,31] as experiments were performed at only one applied magnetic field strength, with $B_0 \leq 9.40$ T. Considering that the known range of La chemical shifts is about 1800 ppm,[19] which is small for a heavy nucleus, and that the maximum CSA is generally of the same order of magnitude as the chemical-shift range of that element, it was expected that

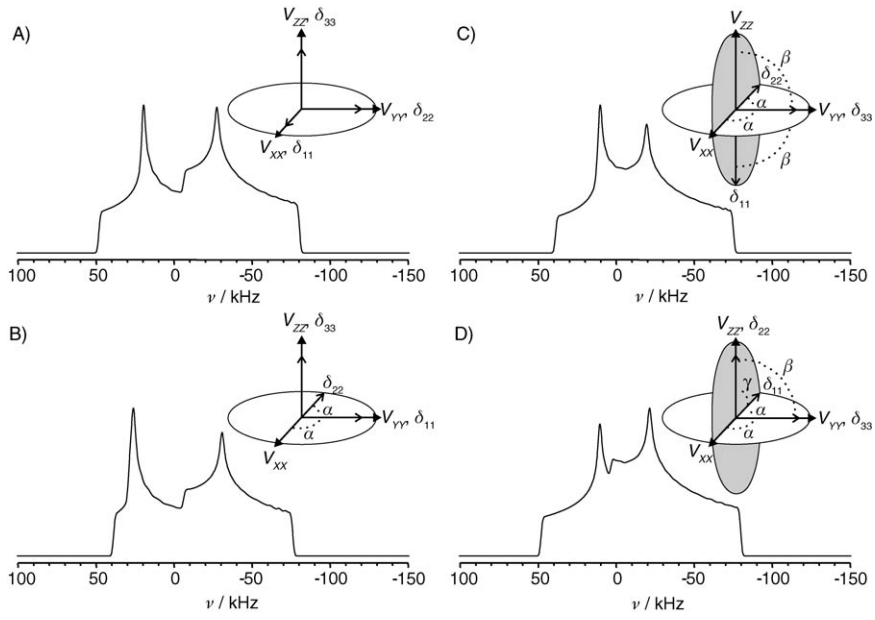

Figure 1. Theoretical ^{139}La solid-state NMR spectra of the central transition, $m_I = {}^1/_2 \leftrightarrow m_I = -{}^1/_2$, of a stationary sample at $B_0 = 17.60$ T. In this example, the EFG tensor is described by $C_Q = 25$ MHz, $\eta_Q = 0.5$, and the chemical-shift tensor is described by $\delta_{iso} = 0$ ppm, $\Omega = 175$ ppm, and $\kappa = 0$. The three Euler angles (α, β, and γ) that describe the counter-clockwise (right-handed) rotations needed to relate the orientations of the tensors are shown in the insets. A) The tensors are coincident and $\alpha = \beta = \gamma = 0°$. B) Rotation about the initial z axis (V_{ZZ}) by α; $\alpha = 90°$, $\beta = \gamma = 0°$, C) followed by a rotation about the new y axis (δ_{22}) by β; $\alpha = \beta = 90°$, $\gamma = 0°$, D) followed by a rotation about the new z axis (δ_{11}) by γ; $\alpha = \beta = \gamma = 90°$.

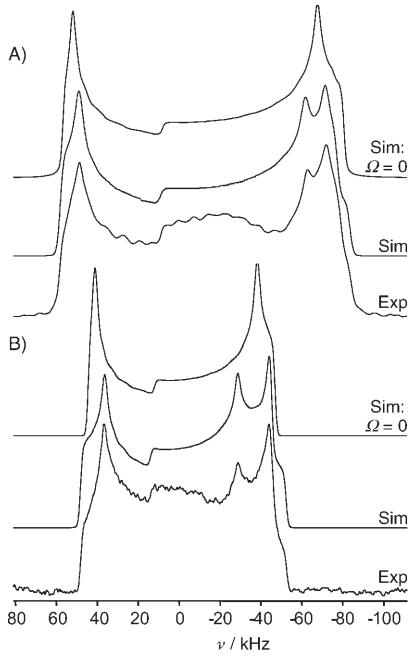

Figure 2. Experimental and simulated ^{139}La solid-state NMR spectra of a stationary sample of $[La(mal)_2(H_2O)_2]\cdot H_2O$ (**4**) at applied magnetic fields of A) 11.75 T and B) 17.60 T. The upper spectrum at each field represents simulations excluding the effects of chemical-shift anisotropy.

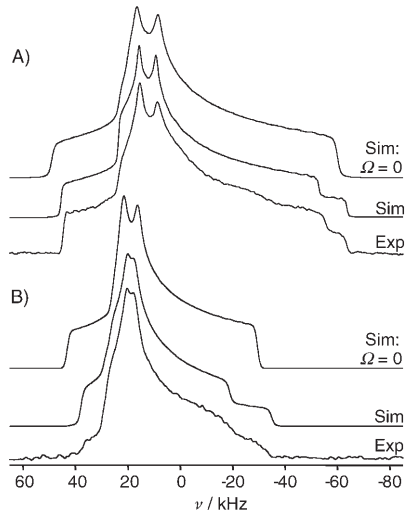

Figure 3. Experimental and simulated ^{139}La solid-state NMR spectra of a stationary sample of $[La(phen)_2(NO_3)_3]$ (**5**) at applied magnetic fields of A) 11.75 T and B) 17.60 T. The upper spectrum at each field represents simulations excluding the effects of chemical-shift anisotropy.

the CSA in these compounds would be small. Thus, at these low applied magnetic fields, the effects of chemical-shift anisotropy on the second-order quadrupolar lineshapes are not obvious and higher applied magnetic field strengths are needed to characterize the ^{139}La CSA. The influence of CSA on the shape of the ^{139}La NMR spectra acquired in this study will be discussed below, followed by an analysis of the relationship between ^{139}La NMR parameters and molecular structure.

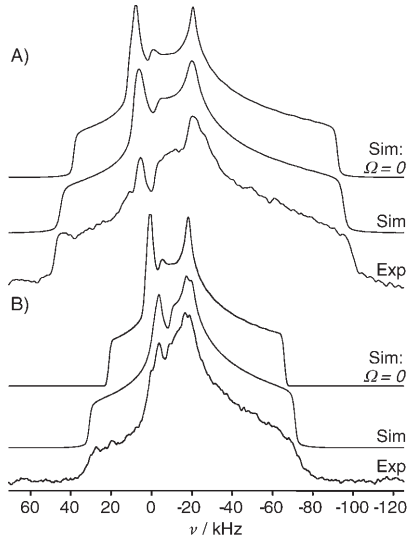

Figure 4. Experimental and simulated ^{139}La solid-state NMR spectra of a stationary sample of $[La([15]crown-5)(NO_3)_3]$ (**8**) at applied magnetic fields of A) 11.75 T and B) 17.60 T. The upper spectrum at each field represents simulations excluding the effects of chemical-shift anisotropy.

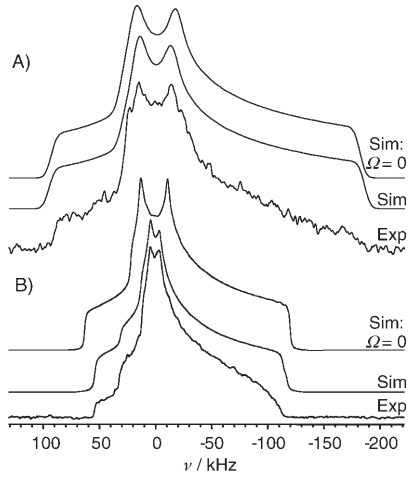

Figure 5. Experimental and simulated ^{139}La solid-state NMR spectra of a stationary sample of $[La(N\text{-macro})(NO_3)_3]$ (**10**) at applied magnetic fields of A) 11.75 T and B) 17.60 T. The upper spectrum at each field represents simulations excluding the effects of chemical-shift anisotropy.

At $B_0 = 11.75$ T, the effect of CSA on the central transition ^{139}La NMR lineshape, albeit small, is distinctive. Specifically, the Euler angles have a dramatic influence upon the shape of the powder patterns, resulting in the addition of discontinuities and shoulders as demonstrated in Figures 2–5. For instance, the spectra of **4** are shown in Figure 2 in which the CSA results in a splitting of the low-frequency discontinuity. For **5** (Figure 3), the inclusion of CSA gives rise to a step in the low-frequency shoulder and a reduction of the high-frequency shoulder while the CSA in **8** (Figure 4) decreases the intensity of the high-frequency discontinuity and causes an overall increase in the breadth of

Table 2. ^{139}La NMR parameters for the compounds included in this study as obtained from simulations of the experimental spectra.[a]

	Compound	EFG parameters		Magnetic-shielding parameters			Euler angles		
		C_Q [MHz]	η_Q	δ_{iso} [ppm]	Ω [ppm]	κ	α [°]	β [°]	γ [°]
1	$[La(acac)_3(H_2O)_2]$	23.5(3)	0.81(2)	120(5)	180(20)	0.35(10)	10(5)	30(15)	0(5)
2	$[La(bipyO)_4(ClO_4)_3]$[b]	35.6(2)	0.05(3)	165(10)	$\leq$125	–	–	–	–
3	$[La(Ph_2MePO)_3(NO_3)_3]$	10.0(1)	0.93(1)	90(5)	50(10)	−0.4(2)	50(20)	75(15)	90(20)
4	$[La(mal)_2(H_2O)_2]\cdot H_2O$	26.1(1)	0.075(15)	114(5)	170(10)	−1.0(2)	80(5)	60(5)	42(5)
5	$[La(phen)_2(NO_3)_3]$	17.90(5)	0.890(5)	178(5)	160(10)	−0.9(1)	55(5)	58(2)	20(5)
6	$[La(glut)_2(H_2O)]\cdot H_2O$	20.85(5)	1.000(5)	10(3)	145(10)	−0.15(2)	19(4)	42(5)	78(10)
7	$[La(teg)(NO_3)_3]$	23.9(2)	0.04(1)	−70(5)	250(20)	0.3(2)	0(30)	2(2)	0(30)
8	[La([15]crown-5)$(NO_3)_3$]	20.6(5)	0.70(3)	−80(5)	150(20)	−1.0(3)	10(5)	6(3)	0(5)
9	[La([18]crown-6)$(NO_3)_3$]	26.5(1)	0.81(1)	−165(5)	170(10)	0.4(1)	30(5)	3(3)	50(5)
10	[La(N-macro)$(NO_3)_3$]	29.0(1)	0.81(1)	20(5)	260(10)	−1.0(4)	90(5)	90(5)	0(1)

[a] Values in parenthesis represent the uncertainty in the simulation parameters. [b] Due to the large C_Q, the Ω and κ values could not be assigned.

the spectrum. Only a slight decrease in the distance between the two discontinuities is observed due to CSA in **10** (Figure 5). The wide variety of Euler angles, not the values of Ω and κ, predominantly account for CSA effects on the lineshapes observed in this study (see Figure 1).

Due to the dependence of the magnetic shielding and quadrupolar interactions on magnetic field strength, the contribution of CSA to both the breadth and shape of solid-state NMR spectra is much more distinct at higher magnetic field strengths. An excellent example of this is illustrated in Figure 5; at $B_0 = 11.75$ T, the effect of CSA on the NMR spectrum of **10** is slight, but at $B_0 = 17.60$ T, the anisotropy results in an additional high-frequency shoulder and *reduces* the breadth of the powder pattern. The squeezing of the middle discontinuities, as observed at the moderate applied magnetic field, is more dramatic at high field. Similarly, CSA has a small effect on the NMR spectrum of **8** at $B_0 =$ 11.75 T, but is clearly manifested at $B_0 = 17.60$ T (Figure 4). Analysis of the data acquired at both applied magnetic fields conclusively demonstrates that, with the possible exception of **2**, all compounds exhibit CSA. Due to the very large C_Q in **2**, it was not possible to unambiguously determine CSA parameters for this compound.

As a result of the large breadths of the experimental NMR spectra, the lineshapes suffer from some spectral distortions, a consequence of nonuniform excitation of the randomly oriented crystallites of the powder sample by the radiofrequency pulse. When the spectra are dominated by the quadrupolar interaction, as in this study, the consequences of the nonuniform excitation depend on the value of η_Q. For compounds with η_Q near 1, the intensity of the high- and low-frequency extremes may be too low, as evident in Figures 3–5 at $B_0 = 17.60$ T. As shown in Figure 2, for compounds with η_Q near 0, there can be a "hole" in the spectrum to the left of the low-frequency discontinuity. Such distortions are commonly observed in the solid-state NMR spectra of half-integer quadrupolar nuclei.[49] The simulation of NMR spectra with lineshape distortions must be approached with caution. If proper experimental and processing techniques are employed and one understands the cause of the distortion, meaningful NMR parameters may be extracted from simulations by aligning the major features of the experimental spectra.

As illustrated in Table 2 and discussed above, both the chemical-shift and EFG tensors can be characterized by analyzing the stationary sample solid-state NMR spectra of a half-integer quadrupolar nucleus such as ^{139}La. One of the goals of this investigation was to examine possible relationships between ^{139}La NMR parameters and molecular/electronic structure. For instance, correlations between metal nuclide NMR parameters and metal coordination number have been made.[22] Thus, plots of select ^{139}La parameters with respect to the La coordination number are presented in Figure 6. From analysis of the plots, there is no discernable relationship between the La coordination number and the relative magnitudes of C_Q and Ω. Regardless, for compounds that have the same coordination number and are comprised of only oxygen-donating ligands, there appears to be a relationship between the relative magnitudes of the ^{139}La C_Q and Ω values; the larger the C_Q value, the greater the Ω value. This conclusion is not too surprising given that the magnitude of both the C_Q and the Ω are typically interpreted based on the symmetry about the NMR nucleus[50–52] and not the coordination number. For example, if the metal is at a site with tetrahedral or octahedral symmetry, the EFG and Ω of the central atom will be zero but for a metal in a square-planar 4-coordinate complex, the EFG and Ω will be nonzero and significant.

The isotropic chemical shifts (δ_{iso}) depend on coordination number, as indicated in Figure 6C. For the oxo complexes, the La nucleus becomes more shielded as the La coordination number increases. The line shown in Figure 6C is a best linear fit of the data and denotes this proposed trend. Similarly, in Al–O environments ^{27}Al becomes more shielded as the Al coordination number increases.[22] This relationship between δ_{iso} and the La coordination number can be used to estimate the coordination number in complexes in which single-crystal X-ray diffraction data is unavailable or ambiguous. For example, in **4** there are ten oxygen atoms about La, one of which has an La–O distance of 2.808 Å, much longer than the average La–O distance of 2.587 Å for the other nine atoms. In the paper describing the crystal structure,[36] the authors considered the compound to have a coordination number of ten although they state that "The La–O(4^b) distance is considerably longer than the others and it may be difficult to decide whether or not La–O(4^b) is a

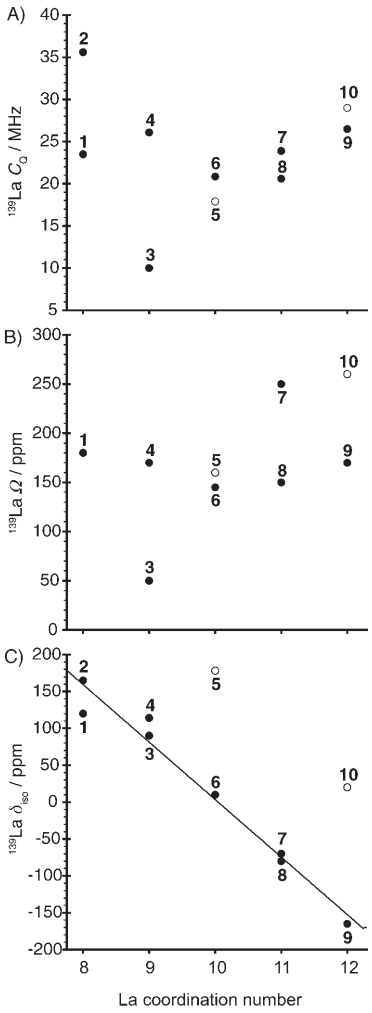

Figure 6. Relationship between the La coordination number and the experimental ^{139}La A) quadrupolar coupling constants (C_Q), B) spans of the chemical-shift tensors (Ω), and C) isotropic chemical shifts (δ_{iso}). The filled circles (●) represent compounds in which the La has only oxygen atoms in its first coordination sphere whereas the open circles (○) represent compounds in which the La has both oxygen and nitrogen atoms in its first coordination sphere. The numbers above the symbols refer to the compound number as indicated in Table 1. The line in C) demonstrates the relationship between the La coordination number (CN) and the ^{139}La isotropic chemical shift in ppm, $\delta_{iso} = 782.9 - (77.9/CN)CN$ ($R^2 = 0.97$), for the compounds containing only oxygen-donating ligands.

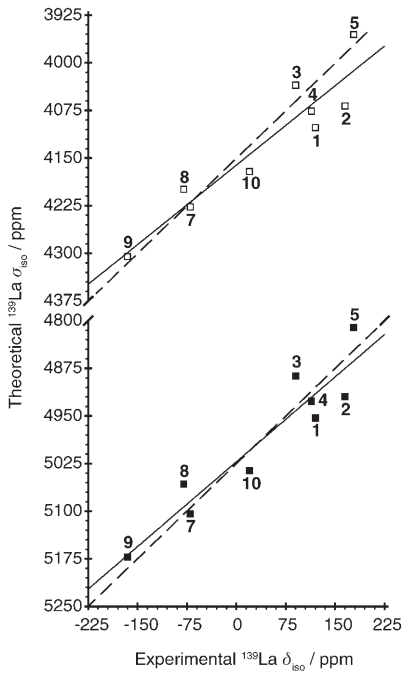

Figure 7. Plot of the ZORA-DFT theoretical ^{139}La isotropic magnetic-shielding constants (σ_{iso}) incorporating scalar (□) or scalar plus spin–orbit (■) relativistic effects versus experimental isotropic chemical shifts (δ_{iso}). The shift and shielding parameters are plotted in the order of decreased shielding. The solid lines, $\sigma_{iso} = 4161 - 0.8342\delta_{iso}$ for the scalar-only and $\sigma_{iso} = 5022 - 0.8909\delta_{iso}$ for the scalar plus spin–orbit data, were determined from the best linear fit of the data. The dashed lines have a slope of minus one and represent ideal agreement between theory and experiment. Data labels refer to the compound number as indicated in Table 1.

bond." Based on the observed ^{139}La δ_{iso} value, it is reasonable to assume that this is not a bond and **4** should be described as a nine-coordinate compound; this coordination geometry is best described as monocapped square antiprism. For the compounds containing both O- and N-donating ligands, the La nucleus is less shielded than in the oxo complexes of the same coordination number. For example, δ_{iso} of **10**, which has six La–N bonds, is 185 ppm greater than δ_{iso} for **9**. This demonstrates that δ_{iso} depends on both the nature of the ligand and the number of bonding atoms.

ZORA-DFT magnetic-shielding calculations: Isotropic magnetic-shielding constants (σ_{iso}) calculated by using the ZORA-DFT method agree qualitatively with the experimental isotropic chemical shifts, δ_{iso} (Figure 7). Perfect agreement between the relative shifts obtained from experiment and theory would result in a line with a slope of -1 (dashed lines). Overall, a linear fit of the data from spin–orbit relativistic calculations (lower solid line) was performed and yields a slope of -0.8909 ($R^2 = 0.89$) whereas the fit of the scalar-only data (upper solid line) yields a line with slope of -0.8342 ($R^2 = 0.88$). The y intercepts of 5022 and 4161 ppm for the spin–orbit and scalar-only calculations, respectively, correspond to the absolute magnetic-shielding constant of aqueous 1.0 M $LaCl_3$ that could hypothetically be used to convert shielding constants to chemical-shift values when using the ZORA-DFT method. The inclusion of spin–orbit coupling results in σ_{iso} values that are on average 860 ppm more shielded than those calculated with only scalar relativistic effects. When calculating only relative isotropic magnetic-shielding constants, however, the inclusion of only scalar relativistic effects is sufficient to obtain good agreement with experimental chemical shifts.

The proposed trend that La is shielded as one adds more oxygen atoms to the first La coordination sphere is generally supported by the calculations. If we consider the compounds that contain only O-donating ligands, **9** is a 12-coordinate complex and is the most shielded, followed by **7** and

8 (11-coordinate), and **4** and **3** (9-coordinate). The calculations predict that the La shielding for **3** and **4** is very similar, further evidence that **4** should be considered a 9-coordinate complex rather than a 10-coordinate complex (see above). The proposed trend, however, is not suitable for the 8-coordinate complexes; the La atom of **1** is more shielded than both of the 9-coordinate complexes, whereas in **2** La is more shielded than in **3**. Thus, either the apparent trend is simply fortuitous or the calculations have a systematic deviation for the 8-coordinate compounds. In addition, because σ_{iso} is an average of the three principal components of the magnetic-shielding tensor, errors in the individual components can potentially cancel and, although individual components may differ significantly from experiment, values of σ_{iso} may agree with experiment. Thus, in order to more thoroughly assess the quality of the magnetic-shielding calculations, one must examine the entire calculated magnetic-shielding tensor.

In addition to δ_{iso}, the remaining parameters that may be used to describe the magnetic-shielding tensor are the span (Ω) and the skew (κ). Unlike theoretical La σ_{iso} values, the theoretical Ω and κ values can be directly compared to experiment. The theoretical span values are about twice as large as the experimental values, with scalar and spin–orbit calculations providing similar results (Table 1 in the Supporting Information). Regardless of this, the general trend is reproduced, the only exception being that the calculated Ω for **5** is smaller than the experimental value. The calculated skew values are more sensitive to the type of relativistic correction included than are the calculated span values. Four of the nine calculated skew values change significantly upon the inclusion of spin–orbit coupling; in all of these cases, the calculated κ improves in comparison with values calculated when only scalar relativistic effects are included. With the incorporation of spin–orbit relativistic effects, six of the eight calculated skew values are within or very close to experimental uncertainties. To conclude, the ZORA-DFT calculations qualitatively reproduce the chemical-shift tensor, with slight overall improvement when spin–orbit relativistic effects are included.

ZORA-DFT EFG calculations and tensor orientations: In general the calculated EFG parameters do not agree well with experiment (Table 1 in the Supporting Information), with scalar-only and spin–orbit calculations providing similar results. Of the compounds studied, only for **2** and **8** are both of the experimental quadrupolar parameters reproduced; the C_Q within 10% of the experimental values and the η_Q within 0.2. As the EFG depends on long-range (intermolecular) interactions in the solid state,[53] the poor performance of the calculations may be a result of the calculations being carried out on isolated molecules. DFT calculations of the EFG in a variety of gaseous scandium(I) diatomics, for which intermolecular effects do not influence the EFG, reproduce the largest component of the EFG tensor about Sc.[54] The average deviation from experiment reported in that study was 13%, much smaller than the average 41% deviation in our calculations. Plane-wave DFT EFG calculations that consider extended structures have been shown to provide accurate values of V_{ZZ} for Sc[55,56] and Gd.[57] The calculated ^{139}La C_Q value in $LaBr_3$ is much closer to experiment when the periodic nature of the salt is incorporated than the value calculated from an isolated fragment.[32] However, the majority of plane-wave EFG calculations have been performed on ionic compounds and whether such calculations can improve calculated EFG parameters in La coordination compounds remains to be investigated.

From NMR experiments on powder samples, one obtains only the relative orientations of the shielding and EFG tensors. The orientation of these tensors in the molecular frame can be determined by symmetry if the compound has axial symmetry, or in systems of lower symmetry, one can use EFG and magnetic-shielding calculations to propose tensor orientations. The only compound in this study with near axial symmetry is **2**. The bipyridine oxide ligands in this compound arrange themselves about the La in such a way that a molecular pseudoplane is formed along the [101] crystallographic plane (Figure 8A). The bonded oxygen atoms of each of the bidentate ligands are oriented perpendicular to this plane, on top of one another. Thus, the molecule has a pseudo-C_4 symmetry axis and the largest component of the EFG tensor, V_{ZZ}, and the unique component of the chemical-shift tensor must be along this axis. The magnetic-shielding calculation predicts that κ is near $+1$ and thus the unique component of the latter tensor is δ_{33}. As η_Q is nearly

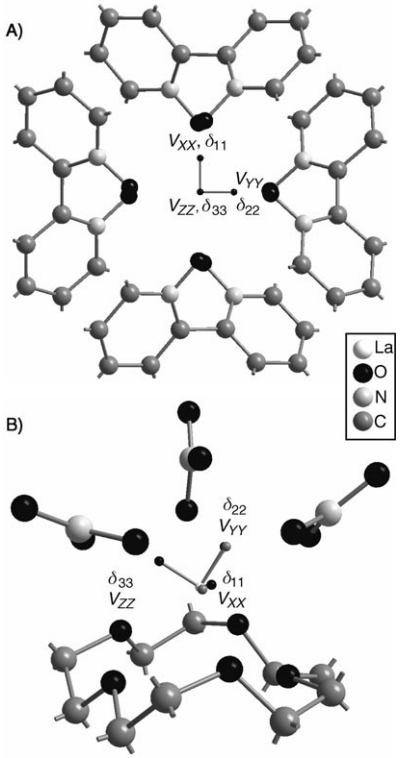

Figure 8. Orientation of the EFG and chemical-shift tensors (A) for **2**, based on symmetry, and (B) for **8**, by using ZORA-DFT magnetic-shielding calculations and experimental Euler angles. For clarity, H atoms and La–O bonds are not shown.

zero, the remaining components of the EFG tensor, (V_{XX} and V_{YY}) are essentially equal in magnitude, must be perpendicular to V_{ZZ}, and likely point directly towards the oxygen atoms of the bipyridine oxide ligands. Even though it is unknown whether the experimental chemical-shift tensor is also axially symmetric, the symmetry of the molecule dictates that δ_{11} and δ_{22} are oriented in the same direction as V_{XX} and V_{YY}. The magnetic-shielding calculations confirm the orientation of the chemical-shift tensor.

For the remaining compounds, the La magnetic-shielding tensor, which depends predominantly on local structure, is adequately described by the ZORA-DFT method. Thus it is reasonable to assume that the orientation of the principal components of the chemical-shift tensor from the calculations are trustworthy. The poor performance of the EFG calculations suggests that the orientation of the EFG tensor cannot be assigned by ZORA-DFT calculations. Because the relative orientations of the chemical-shift and EFG tensors, described by the Euler angles, are known experimentally, the orientation of the EFG tensor in the molecule can be deduced. A good example of this is **8**, as this compound has no obvious symmetry elements and the calculated Ω and κ are within experimental uncertainties. As oriented in Figure 8B, the [15]crown-5 ligand in this compound lies below La while the nitrate ligands lie above La. The chemical-shift tensor components are oriented such that δ_{33} points directly towards one of the bonded O atoms of the nitrate ligands, δ_{22} bisects the other two nitrate ligands, and δ_{11} is parallel to the "planes" of the nitrate ligands and [15]crown-5. The Euler angles dictate that the EFG and chemical-shift tensors are nearly coincident and thus it is relatively simple to determine the orientation of the EFG tensor in this compound.

Conclusion

Several lanthanum(III) coordination compounds, which have coordination numbers ranging from 8 to 12 and are comprised of mixtures of various oxygen- or nitrogen-donating unidentate and/or polydentate ligands, have been studied for the first time by means of solid-state ^{139}La NMR spectroscopy. In all cases, the breadth and shape of the central transition of the ^{139}La NMR spectra of stationary powder samples are dominated by the second-order quadrupolar interaction. The measured ^{139}La C_Q values range from 10.0 MHz for **3** to 35.6 MHz for **2** whereas η_Q is near either 0 or 1 for the compounds studied. Although the NMR spectra are dominated by the quadrupolar interaction, the lineshapes of the NMR spectra are influenced by CSA, particularly the relative orientation of the chemical-shift and EFG tensors. The ^{139}La δ_{iso} value was shown to be related to the La coordination number, such that ^{139}La becomes more shielded as the La coordination number increases.

Relativistic ZORA-DFT calculations of the isotropic magnetic-shielding constants (σ_{iso}) agree qualitatively with the experimental isotropic chemical-shift constants (δ_{iso}). Calculated values of $\sigma_{iso,}$ which include spin–orbit contributions, are on average 860 ppm more shielded than calculations incorporating only scalar relativistic corrections. The calculated Ω is unaffected by the type of relativistic correction included, however, the κ of the shielding tensor is improved upon the inclusion of spin–orbit coupling. The orientation of the chemical-shift tensor within the molecule can be proposed from the magnetic-shielding calculations and, in combination with the experimental Euler angles, can be used to suggest the orientation of the EFG tensor.

This study demonstrates that ^{139}La solid-state NMR spectroscopy of La coordination compounds is feasible and that ^{139}La NMR experiments, even at a moderate magnetic field, can be routine. To analyze the CSA in these compounds NMR spectra must be acquired at a minimum of two applied magnetic fields, one of which should be of a high field strength ($\geq$14.10 T). As shown here, the parameters obtained from the analysis of ^{139}La NMR spectra can provide information about molecular structure and further research investigating the relationship between the ^{139}La NMR parameters and molecular structure in La coordination compounds is encouraged.

Experimental Section

Synthesis: All compounds, except [La(acac)$_3$(H$_2$O)$_2$], which was purchased from Aldrich, were synthesized according to published procedures.[33–42] Where applicable, IR spectroscopy, ^{1}H, ^{13}C, and/or ^{31}P solution NMR spectroscopy, and/or X-ray powder diffraction were performed to verify the purity and identity of the compounds.

Solid-state NMR spectroscopy: Solid-state NMR experiments were performed on stationary powder samples by using standard (90°(X)–τ_1–90°(Y)–τ_2–acquire) or (90°(X)–τ_1–180°(X)–τ_2–acquire) echo pulse sequences, employing either continuous-wave or two-pulse phase modulation (TPPM)[58] ^{1}H decoupling during acquisition. The interpulse delay, τ_1, was set to 30 μs at B_0=11.75 T and 20 μs at B_0=17.60 T and the acquisition delay, τ_2, was set at less than τ_1 to ensure that the top of the echo was acquired. Spectra were processed by left-shifting the free induction decay (FID) to the top of the echo before calculating the frequency domain spectrum by Fourier transformation. Chemical shifts were referenced with respect to a 1.0 M aqueous solution of $LaCl_3$ (0.0 ppm) and pulse widths used for experiments on solids were obtained by dividing the solution 90° pulse by ($I+^1/_2=4$). A one second recycle delay was used for all experiments.

NMR spectra were obtained on a Bruker Avance spectrometer operating at an applied magnetic field of 11.75 T ($\nu_L(^1H)$=500.4 MHz, $\nu_L(^{139}La)$=70.7 MHz) by using a Bruker 7 mm magic-angle-spinning (MAS) probe and a 1.45 μs ($\gamma B_1/2\pi$=43.1 kHz) pulse. The number of transients collected ranged from 44612 to 100000. Experiments at B_0=17.60 T ($\nu_L(^1H)$=749.6 MHz, $\nu_L(^{139}La)$=105.9 MHz) were acquired at the Pacific Northwest National Laboratory on a Varian Inova spectrometer using a home-built 5 mm MAS probe and a 1.0 μs ($\gamma B_1/2\pi$=62.5 kHz) pulse. The number of transients collected ranged from 5200 to 44000.

Analytical simulations of experimental NMR spectra were performed by using the program WSOLIDS, which was developed in our laboratory. WSOLIDS incorporates the space-tiling method of Alderman and coworkers for the generation of frequency-domain solid-state NMR powder patterns.[59]

ZORA-DFT calculations: Density functional theory calculations of ^{139}La quadrupolar coupling constants[60] and magnetic-shielding tensors[61] were performed by using the relativistic zeroth-order regular approximation (ZORA) method[62–64] as implemented in the Amsterdam Density Functional software package.[65–67] Either scalar or scalar plus spin–orbit rela-

tivistic corrections were included in calculations that were performed on an 8 processor cluster operating in a LINUX environment. The integration grid was increased from the default values of 4.0, setting *accint* = 5.0 and *accsph* = 6.0. The exchange correlation functional for determining the unperturbed molecular orbitals employed the local-density approximation of Vosko, Wilk, and Nusair,[68] and the generalized gradient approximation of Becke88[69] and Perdew86.[70,71] The ZORA triple-zeta doubly polarized (TZ2P) basis set was utilized on La and all atoms directly bonded to La, and the ZORA double-zeta (DZ) basis set was used for all remaining atoms. Atomic coordinates were generated from single-crystal X-ray data[33–42] by using DIAMOND,[72] ORTEP,[73] or MOLDEN.[74] Calculations of monomeric compounds were performed on one complete molecule in which the crystallographic positions of all non-H atoms were maintained. Positions of the H atoms were modified by changing any C–H bond lengths to 1.08 Å for CH and CH_2 groups and to 1.089 Å for CH_3 groups. Calculations of polymeric **4** were performed on a 154 atom cluster. Unfortunately adequate energy convergence levels could not be reached for calculations performed on polymeric **6**, regardless of cluster size, thus calculated parameters are not reported for this compound.

Acknowledgements

The solid-state NMR group at the University of Alberta (U of A) is thanked for their helpful comments. NMR experiments at $B_0 = 17.60$ T were performed in the Environmental Molecular Sciences Laboratory, a national scientific user facility sponsored by the US Department of Energy's Office of Biological and Environmental Research and located at the Pacific Northwest National Laboratory in Richland, WA. All the EMSL staff, especially Nancy Isern, Jesse Sears, and Joe Ford, are thanked for their assistance and hospitality. The use of Prof. P.N. Roy's (U of A) LINUX cluster, *Plethora*, which was funded by the Canadian Foundation for Innovation (CFI), is greatly appreciated. M.J.W., K.W.F., and K.J.O. would like to thank the Natural Sciences and Engineering Research Council (NSERC) of Canada, the Alberta Ingenuity Fund, and the University of Alberta for post-graduate scholarships. R.E.W. is the holder of a Canada Research Chair in physical chemistry and thanks the NSERC, the CFI, and the University of Alberta for research funding.

[1] T. Moeller, D. F. Martin, L. C. Thompson, R. Ferrús, G. R. Feistel, W. J. Randall, *Chem. Rev.* **1965**, *65*, 1–50.
[2] P. T. Moseley in *Inorganic Chemistry Series Two, Vol. 7* (Ed.: K. W. Bagnall), University Park Press, Baltimore, **1975**, pp. 65–110.
[3] S. P. Sinha, *Struct. Bonding (Berlin)* **1976**, *25*, 69–149.
[4] H. Tsukube, S. Shinoda, *Chem. Rev.* **2002**, *102*, 2389–2403.
[5] C. Liu, M. Wang, T. Zhang, H. Sun, *Coord. Chem. Rev.* **2004**, *248*, 147–168.
[6] A. F. Cockerill, G. L. O. Davies, R. C. Harden, D. M. Rackham, *Chem. Rev.* **1973**, *73*, 553–588.
[7] B. C. Mayo, *Chem. Soc. Rev.* **1973**, *2*, 49–74.
[8] J. A. Peters, J. Huskens, D. J. Raber, *Prog. Nucl. Magn. Reson. Spectrosc.* **1996**, *28*, 283–350.
[9] R. B. Lauffer, *Chem. Rev.* **1987**, *87*, 901–927.
[10] S. Aime, M. Botta, M. Fasano, E. Terreno, *Chem. Soc. Rev.* **1998**, *27*, 19–29.
[11] P. Caravan, J. J. Ellison, T. J. McMurry, R. B. Lauffer, *Chem. Rev.* **1999**, *99*, 2293–2352.
[12] G. A. Molander, *Chem. Rev.* **1992**, *92*, 29–68.
[13] S. Kobayashi, M. Sugiura, H. Kitagawa, W. W. L. Lam, *Chem. Rev.* **2002**, *102*, 2227–2302.
[14] M. Shibasaki, N. Yoshikawa, *Chem. Rev.* **2002**, *102*, 2187–2209.
[15] J. Gromada, J. F. Carpentier, A. Mortreux, *Coord. Chem. Rev.* **2004**, *248*, 397–410.
[16] N. Sabbatini, M. Guardigli, J. M. Lehn, *Coord. Chem. Rev.* **1993**, *123*, 201–228.
[17] J. Kido, Y. Okamoto, *Chem. Rev.* **2002**, *102*, 2357–2368.
[18] R. K. Harris, E. D. Becker, S. M. C. De Menezes, R. Goodfellow, P. Granger, *Pure Appl. Chem.* **2001**, *73*, 1795–1818.
[19] D. Rehder in *Multinuclear NMR* (Ed.: J. Mason), Plenum, New York, **1987**, pp. 479–519.
[20] E. Klaus, A. Sebald, *Magn. Reson. Chem.* **1994**, *32*, 679–690.
[21] A. P. M. Kentgens, *Geoderma* **1997**, *80*, 271–306.
[22] K. J. D. MacKenzie, M. E. Smith, *Multinuclear Solid-State NMR of Inorganic Materials*, Pergamon, Oxford, **2002**, p. 727.
[23] B. Herreros, P. P. Man, J. M. Manoli, J. Fraissard, *J. Chem. Soc. Chem. Commun.* **1992**, 464–466.
[24] T. J. Bastow, *Solid State Nucl. Magn. Reson.* **1994**, *3*, 17–22.
[25] M. Hunger, G. Engelhardt, J. Weitkamp, *Stud. Surf. Sci. Catal.* **1994**, *84*, 725–732.
[26] M. Hunger, G. Engelhardt, J. Weitkamp, *Microporous Mater.* **1995**, *3*, 497–510.
[27] K. J. D. MacKenzie, M. Schmucker, L. Mayer, *Thermochim. Acta* **1999**, *335*, 73–78.
[28] M. Weihe, M. Hunger, M. Breuninger, H. G. Karge, J. Weitkamp, *J. Catal.* **2001**, *198*, 256–265.
[29] O. Lutz, H. Oehler, *J. Magn. Reson.* **1980**, *37*, 261–267.
[30] A. R. Thompson, E. Oldfield, *J. Chem. Soc. Chem. Commun.* **1987**, 27–29.
[31] R. Dupree, M. H. Lewis, M. E. Smith, *J. Am. Chem. Soc.* **1989**, *111*, 5125–5132.
[32] K. J. Ooms, K. W. Feindel, M. J. Willans, R. E. Wasylishen, J. V. Hanna, K. J. Pike, M. E. Smith, *Solid State Nucl. Magn. Reson.* **2005**, published online: August 24 2005, DOI: 10.1016/j.ssnmr.2005.07.002.
[33] T. Phillips, D. E. Sands, W. F. Wagner, *Inorg. Chem.* **1968**, *7*, 2295–2299.
[34] A. R. Al-Karaghouli, R. O. Day, J. S. Wood, *Inorg. Chem.* **1978**, *17*, 3702–3706.
[35] M. Bosson, W. Levason, T. Patel, M. C. Popham, M. Webster, *Polyhedron* **2001**, *20*, 2055–2062.
[36] F. Marrot, J. C. Trombe, *Polyhedron* **1994**, *13*, 1931–1935.
[37] M. Fréchette, I. R. Butler, R. Hynes, C. Detellier, *Inorg. Chem.* **1992**, *31*, 1650–1656.
[38] B. Benmerad, A. Guehria-Laidoudi, F. Balegroune, H. Birkedal, G. Chapuis, *Acta Crystallogr. Sect. C* **2000**, *56*, 789–792.
[39] U. Casellato, G. Tomat, P. Di Bernardo, R. Graziani, *Inorg. Chim. Acta* **1982**, *61*, 181–187.
[40] R. D. Rogers, A. N. Rollins, *J. Crystallogr. Spectrosc. Res.* **1990**, *20*, 389–393.
[41] J. D. J. Backer-Dirks, J. E. Cooke, A. M. R. Galas, J. S. Ghotra, C. J. Gray, F. A. Hart, M. B. Hursthouse, *J. Chem. Soc. Dalton Trans.* **1980**, 2191–2198.
[42] J. D. J. Backer-Dirks, C. J. Gray, F. A. Hart, M. B. Hursthouse, B. C. Schoop, *J. Chem. Soc. Chem. Commun.* **1979**, 774–775.
[43] P. P. Man in *Encyclopedia of Nuclear Magnetic Resonance, Vol. 6* (Eds.: D. M. Grant, R. K. Harris), Wiley, Chichester, **1996**, pp. 3838–3848.
[44] A. J. Vega in *Encyclopedia of Nuclear Magnetic Resonance, Vol. 6* (Eds.: D. M. Grant, R. K. Harris), Wiley, Chichester, **1996**, pp. 3869–3889.
[45] J. T. Cheng, J. C. Edwards, P. D. Ellis, *J. Phys. Chem.* **1990**, *94*, 553–561.
[46] W. P. Power, R. E. Wasylishen, S. Mooibroek, B. A. Pettitt, W. Danchura, *J. Phys. Chem.* **1990**, *94*, 591–598.
[47] J. Mason, *Solid State Nucl. Magn. Reson.* **1993**, *2*, 285–288.
[48] D. S. Rubinoff, C. J. Evans, M. C. L. Gerry, *J. Mol. Spectrosc.* **2003**, *218*, 169–179.
[49] P. R. Bodart, J. P. Amoureux, Y. Dumazy, R. Lefort, *Mol. Phys.* **2000**, *98*, 1545–1551.
[50] O. Knop, E. M. Palmer, R. W. Robinson, *Acta Crystallogr. Sect. A* **1975**, *31*, 19–31.
[51] O. Knop, *Acta Crystallogr. Sect. A* **1976**, *32*, 147–149.
[52] J. W. Akitt, W. S. McDonald, *J. Magn. Reson.* **1984**, *58*, 401–412.
[53] C. P. Slichter in *Principles of Magnetic Resonance*, 3rd ed., Springer, New York, **1990**, pp. 485–502.
[54] R. Bast, P. Schwerdtfeger, *J. Chem. Phys.* **2003**, *119*, 5988–5994.

[55] K. Sato, H. Akai, Y. Maruyama, T. Minamisono, K. Matsuta, M. Fukuda, M. Mihara, *Hyperfine Interact.* **1999**, *121*, 145–149.
[56] H. Haas, *Hyperfine Interact.* **2001**, *136/137*, 731–735.
[57] M. Diviš, K. Schwarz, P. Blaha, G. Hilscher, H. Michor, S. Khmelevskyi, *Phys. Rev. B* **2000**, *62*, 6774–6785.
[58] A. E. Bennett, C. M. Rienstra, M. Auger, K. V. Lakshmi, R. G. Griffin, *J. Chem. Phys.* **1995**, *103*, 6951–6958.
[59] D. W. Alderman, M. S. Solum, D. M. Grant, *J. Chem. Phys.* **1986**, *84*, 3717–3725.
[60] E. van Lenthe, E. J. Baerends, *J. Chem. Phys.* **2000**, *112*, 8279–8292.
[61] G. Schreckenbach, T. Ziegler, *J. Phys. Chem.* **1995**, *99*, 606–611.
[62] E. van Lenthe, E. J. Baerends, J. G. Snijders, *J. Chem. Phys.* **1993**, *99*, 4597–4610.
[63] E. van Lenthe, E. J. Baerends, J. G. Snijders, *J. Chem. Phys.* **1994**, *101*, 9783–9792.
[64] E. van Lenthe, A. Ehlers, E. J. Baerends, *J. Chem. Phys.* **1999**, *110*, 8943–8953.
[65] C. Fonseca Guerra, J. G. Snijders, G. te Velde, E. J. Baerends, *Theor. Chem. Acc.* **1998**, *99*, 391–403.
[66] G. te Velde, F. M. Bickelhaupt, E. J. Baerends, C. Fonseca Guerra, S. J. A. Van Gisbergen, J. G. Snijders, T. Ziegler, *J. Comput. Chem.* **2001**, *22*, 931–967.
[67] ADF2004.01, SCM, Theoretical Chemistry, Vrije Universiteit, Amsterdam (The Netherlands), http://www.scm.com.
[68] S. H. Vosko, L. Wilk, M. Nusair, *Can. J. Phys.* **1980**, *58*, 1200–1211.
[69] A. D. Becke, *Phys. Rev. A* **1988**, *38*, 3098–3100.
[70] J. P. Perdew, *Phys. Rev. B* **1986**, *33*, 8822–8824.
[71] J. P. Perdew, *Phys. Rev. B* **1986**, *34*, 7406–7406.
[72] G. Bergerhoff, M. Berndt, K. Brandenburg, *J. Res. Natl. Inst. Stand. Technol.* **1996**, *101*, 221–225.
[73] ORTEP-III: M. N. Burnett, C. K. Johnson, Oak Ridge Thermal Ellipsoid Plot Program for Crystal Structure Illustrations, Oak Ridge National Laboratory Report ORNL-6895.
[74] G. Schaftenaar, J. H. Noordik, *J. Comput.-Aided Mol. Des.* **2000**, *14*, 123–134.
[75] L. A. Aslanov, M. A. Porai-Koshits, M. O. Dekaprilevich, *Zh. Strukt. Khim.* **1971**, *12*, 470–473.
[76] E. Huskowska, I. Turowska-Tyrk, J. Legendziewicz, J. P. Riehl, *New J. Chem.* **2002**, *26*, 1461–1467.
[77] E. Hansson, *Acta Chem. Scand.* **1973**, *27*, 2441–2454.
[78] E. Hansson, *Acta Chem. Scand.* **1973**, *27*, 2813–2826.
[79] M. Hernández-Molina, P. Lorenzo-Luis, C. Ruiz-Pérez, T. López, I. R. Martín, K. M. Anderson, A. G. Orpen, E. H. Bocanegra, F. Lloret, M. Julve, *J. Chem. Soc. Dalton Trans.* **2002**, 3462–3470.
[80] M. Hernández-Molina, C. Ruiz-Pérez, T. López, F. Lloret, M. Julve, *Inorg. Chem.* **2003**, *42*, 5456–5458.
[81] D. L. Kepert, L. I. Semenova, A. N. Sobolev, A. H. White, *Aust. J. Chem.* **1996**, *49*, 1005–1008.
[82] A. G. Mirochnik, B. V. Bukvetskii, P. A. Zhikhareva, V. E. Karasev, *Russ. J. Coord. Chem.* **2001**, *27*, 443–448.
[83] Y. Q. Zheng, L. X. Zhou, J. L. Lin, S. W. Zhang, *Z. Anorg. Allg. Chem.* **2001**, *627*, 1643–1646.
[84] D. Y. Wei, J. L. Lin, Y. Q. Zheng, *J. Coord. Chem.* **2002**, *55*, 1259–1262.
[85] A. S. Antsyshkina, G. G. Sadikov, M. N. Rodnikova, A. I. Mikhailichenko, L. V. Nevzorova, *Russ. J. Inorg. Chem.* **2002**, *47*, 361–366.
[86] Q. Y. Lin, Y. L. Feng, *Z. Kristallogr. New Cryst. Struct.* **2003**, *218*, 531–532.
[87] T. Głowiak, D. C. Ngoan, J. Legendziewicz, *Acta Crystallogr. Sect. C* **1986**, *42*, 1494–1496.
[88] F. Serpaggi, G. Férey, *J. Mater. Chem.* **1998**, *8*, 2737–2741.
[89] T. Lu, L. Ji, M. Tan, Y. Liu, K. Yu, *Polyhedron* **1997**, *16*, 1149–1156.
[90] V. Alexander, *Chem. Rev.* **1995**, *95*, 273–342.
[91] Y. H. Lin, Y. Xing, *Acta Chim. Sin.* **1983**, *41*, 97–102.
[92] J. C. G. Bünzli, B. Klein, G. Chapuis, K. J. Schenk, *Inorg. Chem.* **1982**, *21*, 808–812.
[93] N. N. McIntosh, I. A. Kahwa, J. T. Mague, *Acta Crystallogr. Sect. E* **2001**, *57*, M21–M22.
[94] R. D. Rogers, A. N. Rollins, *J. Chem. Crystallogr.* **1994**, *24*, 321–329.
[95] F. Vogtle, E. Weber, *Angew. Chem.* **1979**, *91*, 813–837; *Angew. Chem. Int. Ed. Engl.* **1979**, *18*, 753–776.
[96] G. Bombieri, F. Benetollo, A. Polo, L. De Cola, D. L. Smailes, L. M. Vallarino, *Inorg. Chem.* **1986**, *25*, 1127–1132.
[97] A. M. Arif, J. D. J. Backer-Dirks, C. J. Gray, F. A. Hart, M. B. Hursthouse, *J. Chem. Soc. Dalton Trans.* **1987**, 1665–1673.
[98] P. H. Smith, J. R. Brainard, D. E. Morris, G. D. Jarvinen, R. R. Ryan, *J. Am. Chem. Soc.* **1989**, *111*, 7437–7443.

Received: July 6, 2005
Published online: October 13, 2005

